STRUCTURAL SCIENCE
CRYSTAL ENGINEERING
MATERIALS

Volume 77 (2021)

Supporting information for article:

Structure of 1,6-anhydro-β-D-glucopyranose in plastic crystal, orientational glass, liquid and ordinary glass forms: molecular modeling and X-ray diffraction studies Structure of 1,6-anhydro-β-D-glucopyranose in plastic crystal, orientational glass, liquid and ordinary glass forms: molecular modeling and X-ray diffraction studies

Karolina Jurkiewicz, Wojciech Glajcar, Kamil Kamiński, László Temleitner and Andrzej Burian

S1. The determination of pure diffraction profiles using a regularization procedure

Instrumental broadening of measured powder diffraction intensity profiles is the reason for the loss of their resolution. This leads to problems with the precise and reliable analysis of diffraction data. The effect of the instrumental broadening can be described by the convolution equation (Warren, 2014; Hosemann & Bagchi, 1962)

$$I_m(Q) = I(Q) * I_i(Q) = \int_{-\infty}^{\infty} I(Q')I_i(Q - Q')dQ', \quad \text{(S1)}$$

where $I_m(Q)$ is the measured intensity, $I_i(Q)$ denotes the instrument function and $I(Q)$ is the pure diffraction profile. The above equation represents a Fredholm integral equation of the first kind (Arfken, 1985)

$$h(x) = \int_{-\infty}^{\infty} f(y)g(x - y)dy. \quad \text{(S2)}$$

In order to determine the pure diffraction profile, $f(x)$, from the measured and instrumental diffraction profiles, $h(x)$ and $g(x)$, respectively one has to solve the S2 equation.
A reasonable approximation of the instrumental function can be obtained from the measurement of a standard material under the same conditions as for the sample. Several numerical procedures have been used to deconvolute the measured powder x-ray diffraction patterns with the apparatus function (Burger & van Cittert, 1932; Stokes & Wilson, 1942; Stokes, 1948; Jones *et al*. 1967; Ergun, 1968; Howells, 1984; Sánchez-Bajo & Cumbrera, 2000; Ida & Toraya, 2002, Li *et al*. 2016). In this paper the method based on the simple Simpson quadrature (Press *et al*. 1986) and the regularization algorithm (Tikhonov & Arsenin, 1977; Morozov, 1984) is used in order to obtain the pure diffraction profiles for 1,6-anhydro-β-D-glucose. In real x-ray diffraction experiment the integration limits in formulas S1 and S2 are, say a and b. Then equation S2 can be rewritten as

$$h(x) = \int_{a}^{b} f(y)g(x - y)dy. \quad \text{(S3)}$$

Using the Simpson integration rule, the last equation will take the form of a linear system of equations:

$$h(x_1) \cong \frac{\Delta y}{3}[f(y_1)g(x_1 - y_1) + 4f(y_2)g(x_1 - y_2) + 2f(y_3)g(x_1 - y_3) + \cdots$$

$$+2f(y_{n-2})g(x_1 - y_{n-2}) + 4f(y_{n-1})g(x_1 - y_{n-1}) + f(y_n)g(x_1 - y_n)]$$

$$h(x_2) \cong \frac{\Delta y}{3}[f(y_1)g(x_2 - y_1) + 4f(y_2)g(x_2 - y_2) + 2f(y_3)g(x_2 - y_3) + \cdots$$

$$+2f(y_{n-2})g(x_2 - y_{n-2}) + 4f(y_{n-1})g(x_2 - y_{n-1}) + f(y_n)g(x_2 - y_n)]$$

.

.

.

$$h(x_m) \cong \frac{\Delta y}{3}[f(y_1)g(x_m - y_1) + 4f(y_2)g(x_m - y_2) + 2f(y_3)g(x_m - y_3) + \cdots$$

$$+2f(y_{n-2})g(x_m - y_{n-2}) + 4f(y_{n-1})g(x_m - y_{n-1}) + f(y_n)g(x_m - y_n)] \quad \text{(S4)}$$

where Δy is the integration step, $y_1 = a$ and $y_n = b$. In matrix form, this system of equations can be represented as follows

$$h = Af, \quad \text{(S5)}$$

h is a vector with m components representing the measured intensity, g is a vector representing n components of the instrument function and matrix A contains n unknown values of the true intensity function multiplied by the Simpson coefficients and $\Delta y/3$. Applying the linear least-squares method to solve (S5) leads to the matrix equation

$$A^T h = A^T A f, \quad \text{(S6)}$$

where A^T is the transpose matrix of A (Press *et al*. 1986). In principle, the Gauss normal equations (S6) can be solved using the standard methods such as LU decomposition and back-substitution or Gauss-Jordan elimination (Press *et al*. 1986). However, in order to obtain an enough reconstitute solution for f its values have to be very close together that leads to solution instability. In other words, the problem is ill-posed (Varah, 1979). Tikhonov & Arsenin (1977) and Morozov (1979) proposed the regularization method to avoid such a problem. In general, in the least-squares method the Euclidean norm $\|Af - h\|^2$ is minimized. Instead, the regularization procedure is based on the minimization of

$$(\|Af - h\|^2 + \alpha\|Lf\|^2) \quad \text{(S7)}$$

which is, in turn, equivalent to the normal system

$$(A^T A + \lambda L^T L)f = A^T h. \quad \text{(S8)}$$

The regularization parameter α is adjustable and has to be chosen carefully. The criterion for the correctness of its selection may be the compatibility of the obtained solution convoluted with the apparatus function with the measured intensity function. Three different regularization matrices L, namely the identity matrix ($L = I$), the matrix operator of the first ($L = L^1$) and second derivative ($L = L^2$) are used in the regularization algorithm (Varah, 1979). The choices of these three regularization matrices allow controlling the norm of the vector f (the identity matrix) or its first or second derivative, preventing the solution instability. Numerical trials have shown that the more efficient choice is $L = L^2$.

$$L^2 = \begin{pmatrix} 1 & -2 & 1 & \cdots & 0 & 0 & 0 \\ \vdots & & & \ddots & & \vdots & \\ 0 & 0 & 0 & \cdots & 1 & -2 & 1 \end{pmatrix} \quad \text{(S9)}$$

The main idea of the regularization method, expressed in terms of the estimation theory, is that linear unbiased estimation from ill-conditioned data can be greatly improved by the use of slightly biased estimator focusing on small mean-square error rather than least-squares (Hoerl & Kennerd, 1970; Marquardt, 1970).

S2. The pure diffraction profiles for 1,6-anhydro-β-D-glucose

In order to correct for the instrumental broadening in the experimental data of different forms of 1,6-anhydro-β-D-glucose (levoglucosan) the standard Si powder–from NIST (SRM 640e - Line Position and Line Shape Standard for Powder Diffraction) was measured under instrumental conditions identical to those of the sample. The standard polycrystal size 4.1 μm is large enough to make the particle-size broadening negligible. The (111) peak of the standard diffraction pattern was chosen as the instrumental function. At this stage it is necessary to check whether the peak broadening of the instrument response function is Q-dependent as it has been discussed by Toby & Egami (1992). The full

width at half maximum (FWHM) values for the Si standard were estimated using the FITYK software (Wojdyr, 2010) and plotted as a function of Q in figure S2.1.

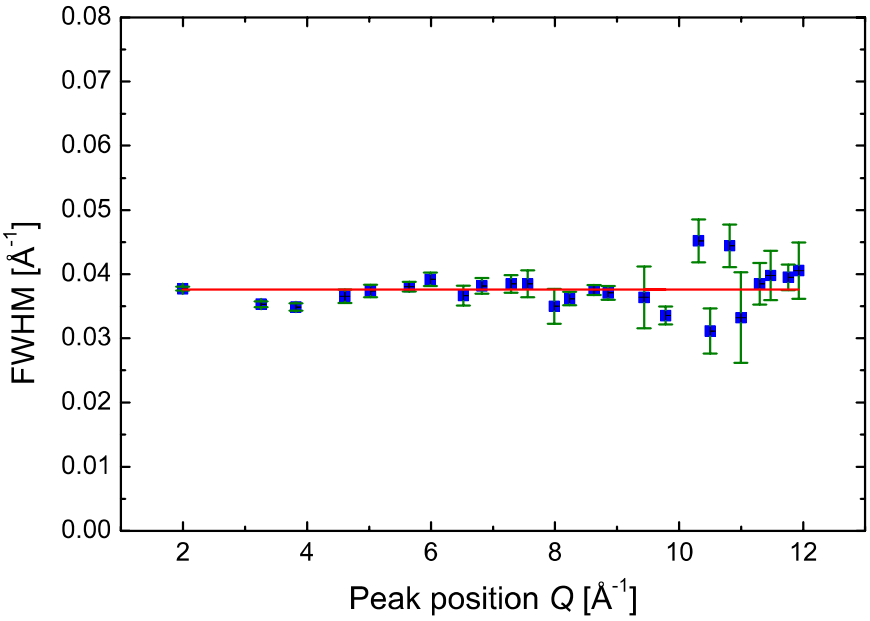

Figure S2.1. FWHM for peak positions of the Si standard (blue squares) together with their uncertainties estimated using the FITYK software.

By analyzing this chart, it can be concluded that within reasonable limits the FWHM values do not change significantly in the whole Q-range and the standard (111) peak can be taken as a good approximation of the apparatus function.

In figure S2.2 the measured intensity of the plastic crystal (PC) form of levoglucosan is compared with the Si standard (111) peak. This comparison shows that the instrumental broadening should be included in further structural analysis. The results of the deconvolution procedure and their tests are shown below in figures S2.3-S2.10. All the deconvolution procedures were performed with the value of the regularization parameter $\alpha = 0.01$.

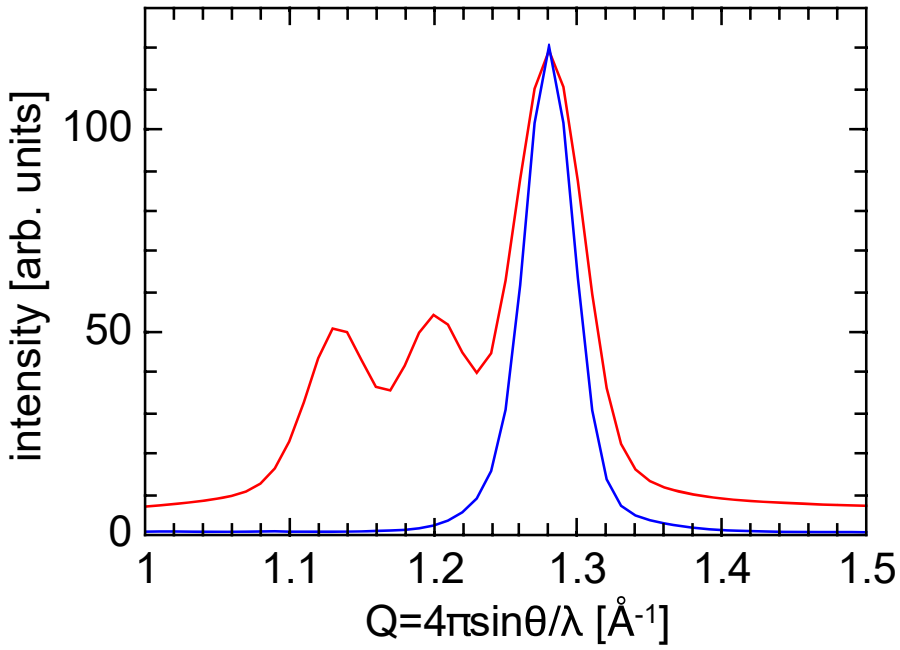

Figure S2.2. The intensity of plastic crystal (PC) form of levoglucosan (red line) and the Si (111) peak (blue line) scaled and shifted to the position of the PC highest peak plotted in the 1-1.5 Å^{-1} Q-range.

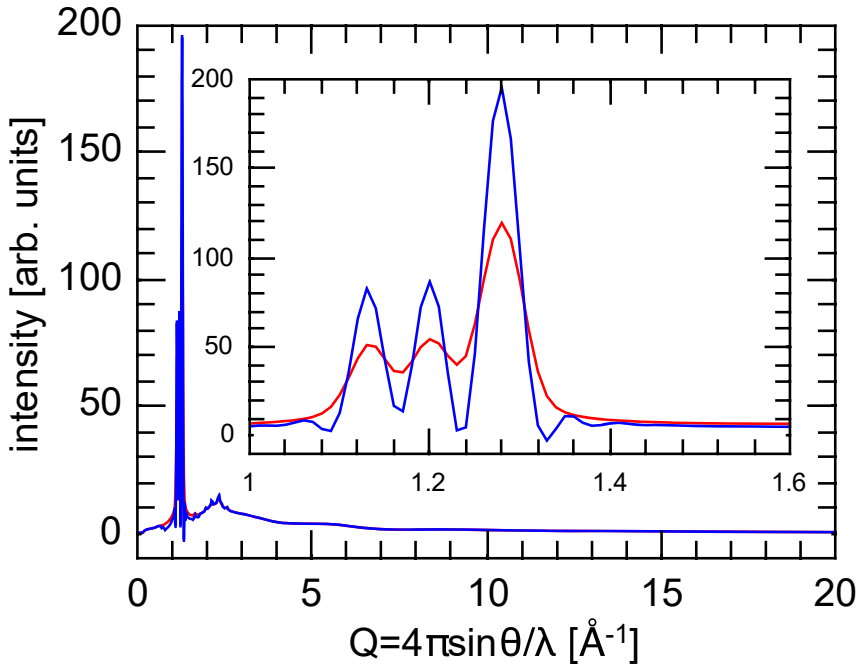

Figure S2.3. The measured intensity (red line) and the deconvoluted intensity (blue line) for the PC sample.

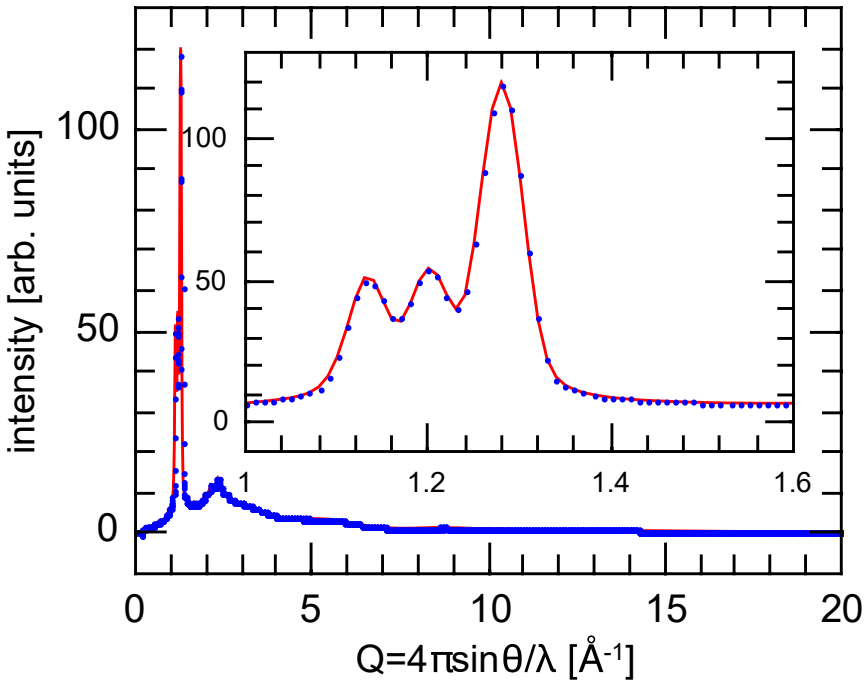

Figure S2.4. The measured intensity (red line) and the back-convoluted intensity (blue circles) for the PC sample.

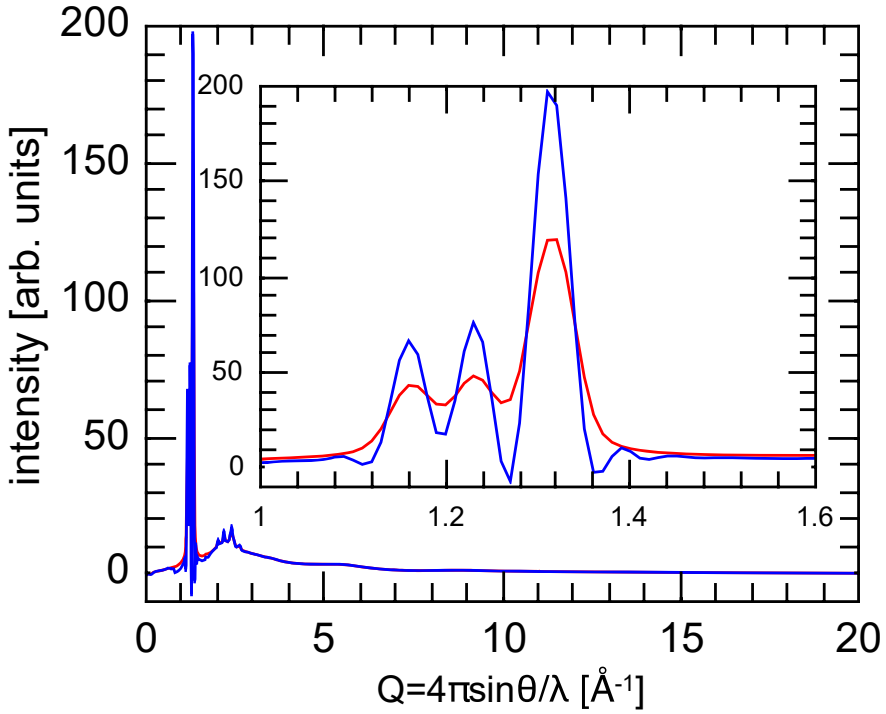

Figure S2.5. The measured intensity (red line) and the deconvoluted intensity (blue line) for the orientational glass (OTG) sample.

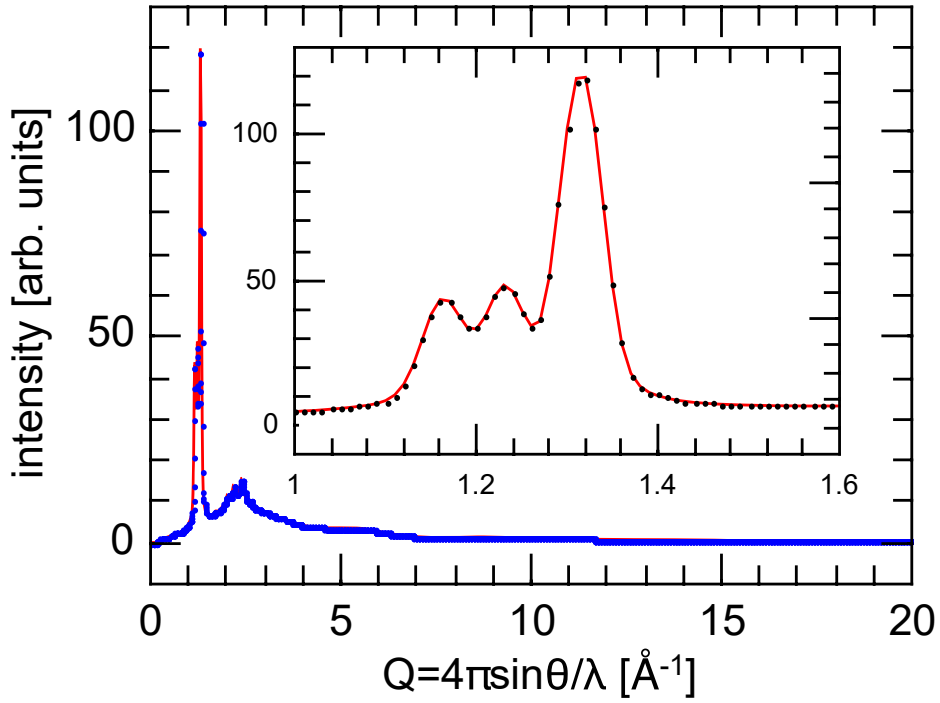

Figure S2.6. The measured intensity (red line) and the back-convoluted intensity (blue circles) for the OTG sample.

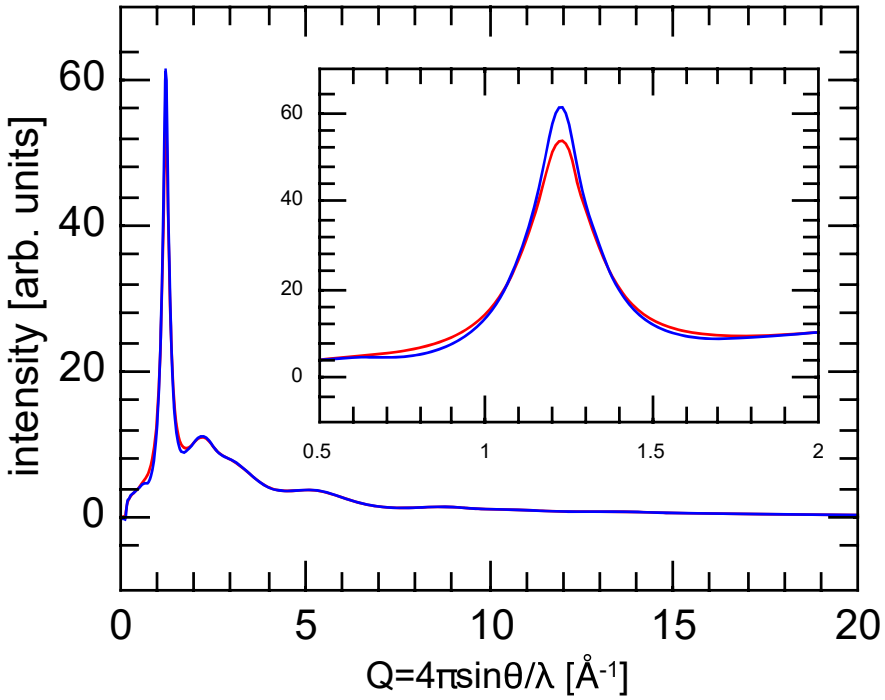

Figure S2.7. The measured intensity (red line) and the deconvoluted intensity (blue line) for the liquid (LQ) sample.

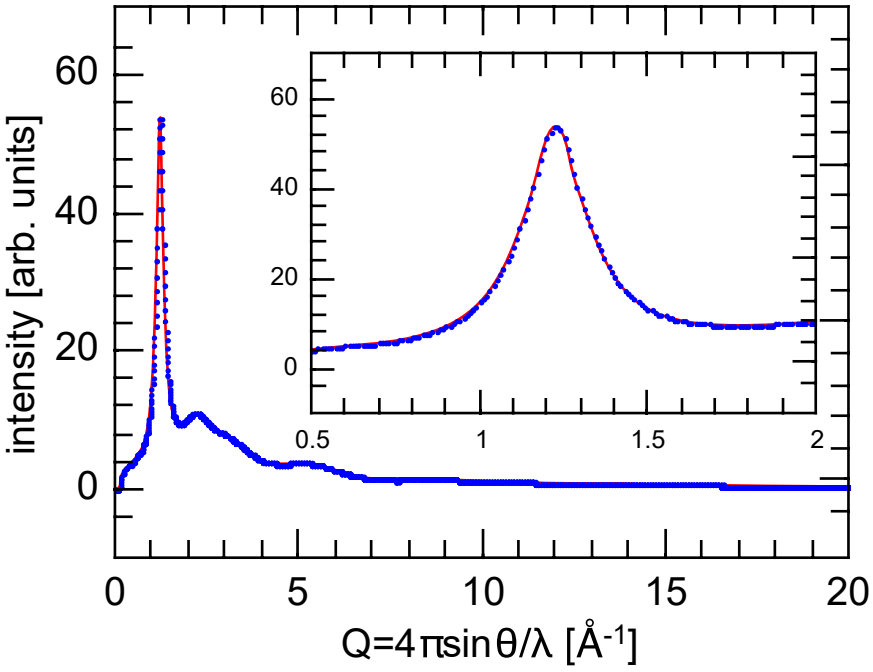

Figure S2.8. The measured intensity (red line) and the back-convoluted intensity (blue circles) for the LQ sample.

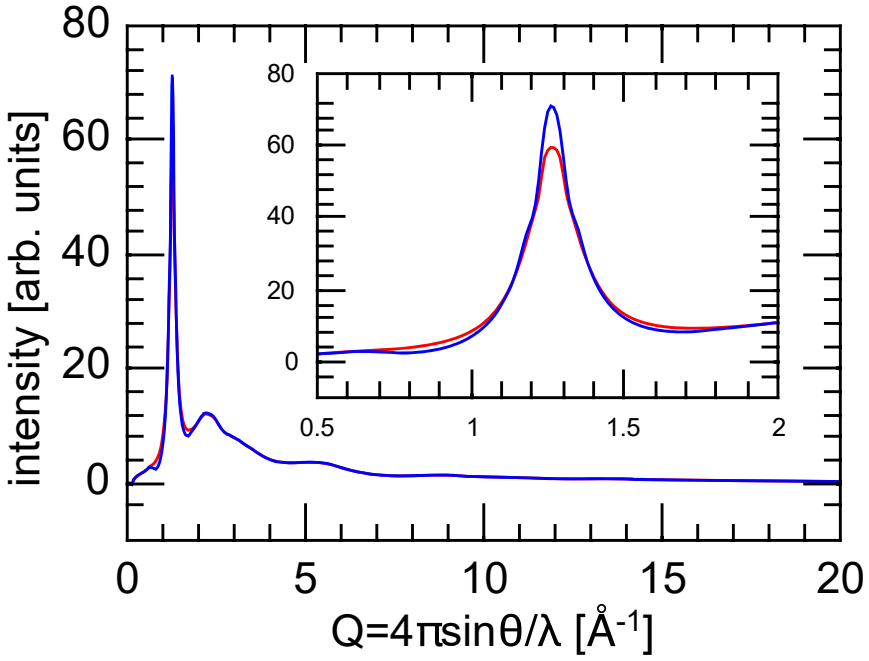

Figure S2.9. The measured intensity (red line) and the deconvoluted intensity (blue line) for the ordinary glass (OG) sample.

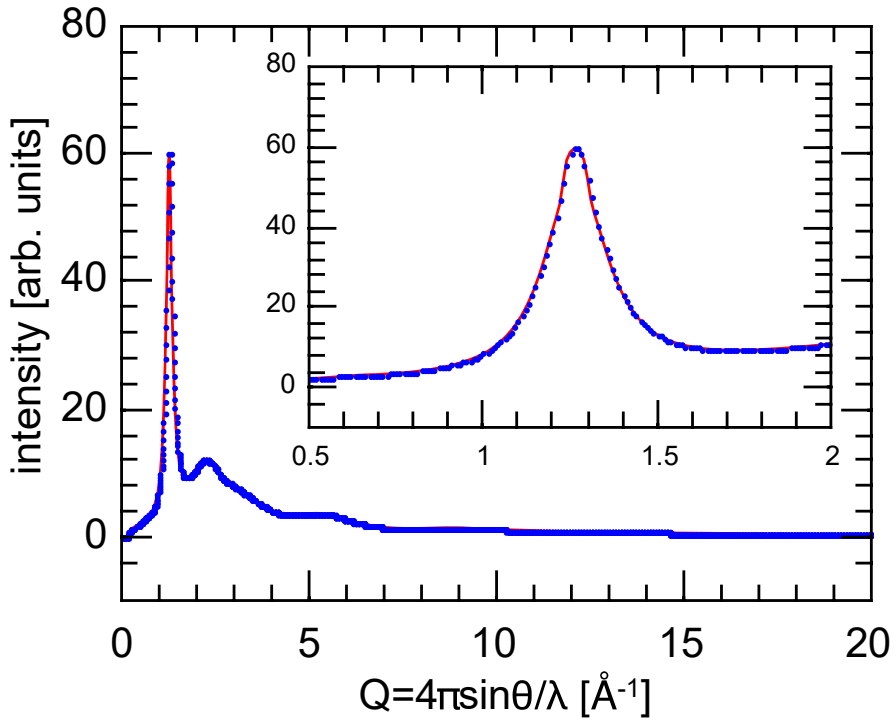

Figure S2.10. The measured intensity (red line) and the back-convoluted intensity (blue circles) for the OG sample.

S3. The hcp model of LQ and OG phases

The first attempt to model the structure of levoglucosan LQ and OG phases was based on the optimization of an average scattering domains with molecules located in the hcp-type network and rotated around their geometrical center, as ahown in the main article for PC and OTG phases. The models of LQ and OG with free rotations of the molecules resulted in the best fits to the experimental data in both reciprocal and real spaces, as in case of PC and OTG.

The lattice parameters a=6.24 Å, c=10.19 Å and a=6.08 Å, c=9.93 Å were taken for computations for LQ and OG, respectively.

The comparison between the model-based and experimental structure factors and atomic pair distribution functions for LQ and OG are shown in figures S3.1 and S3.2, respectively. The parameters of the models are listed in tables S3.1 and S3.2, respectively.

Table S3.1 The hcp model size along the x, y and z axes, respectively, for the LQ phase and the values of the mean square displacements from the equilibrium position for carbon, oxygen and hydrogen atoms.

model size [Å]	$\langle u_C^2 \rangle$ [Å^2]	$\langle u_O^2 \rangle$ [Å^2]	$\langle u_H^2 \rangle$[Å^2]
31.2 × 32.4 × 30.57	0.0025	0.0049	0.0100

Table S3.2 The hcp model size along the x, y and z axes, respectively, for the OG phase and the values of the mean square displacements from the equilibrium position for carbon, oxygen and hydrogen atoms.

model size [Å]	$\langle u_C^2 \rangle$ [Å^2]	$\langle u_O^2 \rangle$ [Å^2]	$\langle u_H^2 \rangle$[Å^2]
54.72 × 52.65 ×49.65	0.0020	0.0042	0.0090

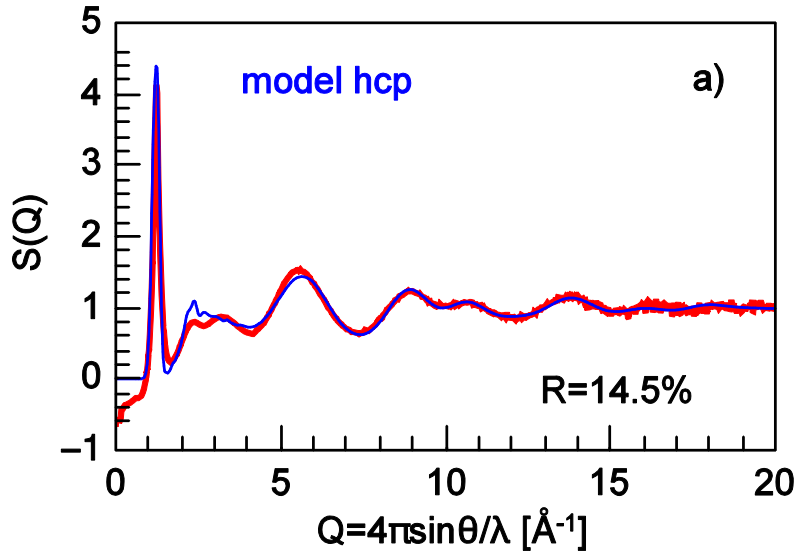

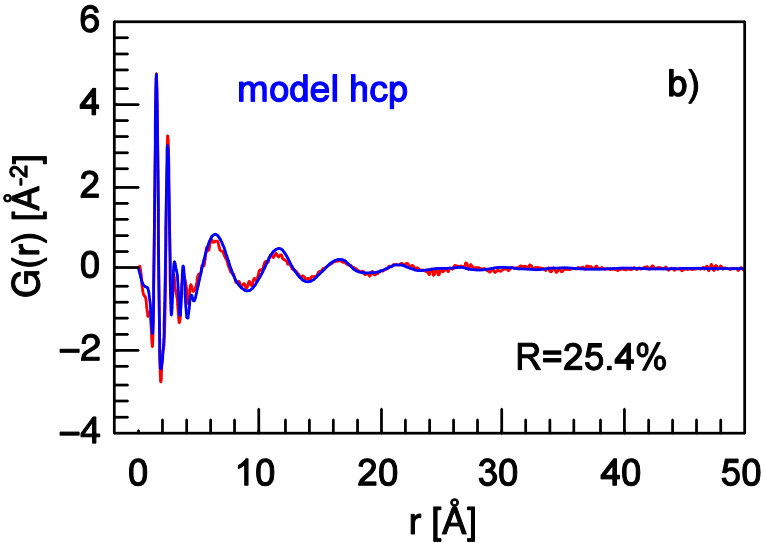

Figure S3.1 A comparison of the static structure factors $S(Q)$ (a) and the pair distribution functions $G(r)$ (b) obtained from the model-based simulations for the hcp system with the experimental data for the LQ phase. Complete randomness of molecular orientations was assumed in the modeling procedure. Additionally, the paracrystalline disorder with the parameters $\sigma^2_{ideal} = 0.0225$ Å^2 and $\sigma^2_{real} = 0.0009$ Å^2 was imposed on the model. The model-based simulations are drawn in blue and the experimental data are plotted in red.

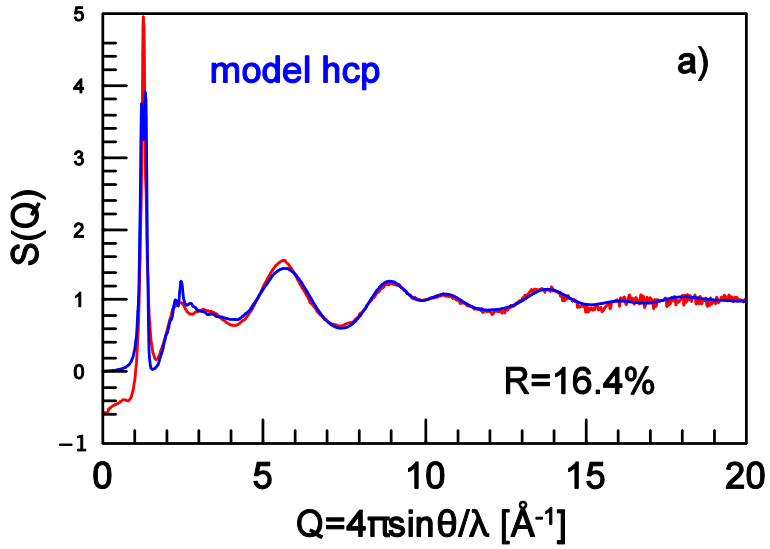

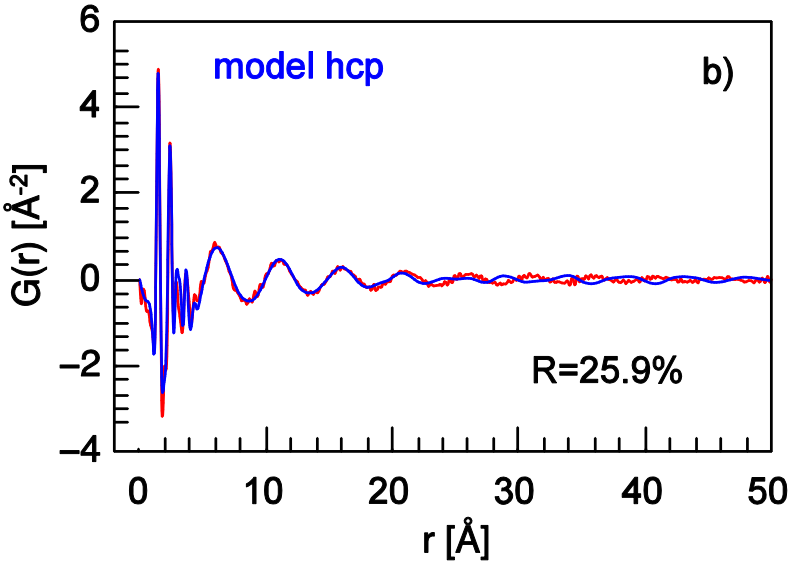

Figure S3.2 A comparison of the static structure factors $S(Q)$ (a) and the pair distribution functions $G(r)$ (b) obtained from the model-based simulations for the hcp system with the experimental data for the OG phase. Complete randomness of molecular orientations was assumed in the modeling procedure. Additionally, the paracrystalline disorder with the parameters $\sigma^2_{ideal} = 0.0324$ Å^2 and $\sigma^2_{real} = 0.0036$ Å^2 was imposed on the model. The model-based simulations are drawn in blue and the experimental data are plotted in red.

References

Arfken, G. (1985). *Mathematical Methods for Physicists*. Orlando: Academic press.

Burger, H.C. & van Cittert P.H. (1932). *Z. Physik*. **79**, 722-730.

Ergun, S. (1968). *J. Appl. Cryst.* **1**, 19-23.

Hoerl, A.E. & Kennard, R.W. (1970). *Technometrics*. **12**, 55-67.

Hosemann, R. & Bagchi, S. N. (1962). *Direct Analysis of Diffraction by Matter*. Amsterdam: North Holland.

Howells, W.S. (1984). *Nucl. Instr. and Meth. in Phys. Res.* **219**, 543-552.

Ida, T. & Toraya, H. (2002). *J. Appl. Cryst.* **35**, 58-68.

Jones, R.N. & Venkataraghavan, R. & Hopkins, J.W. (1967). *Spectrocim. Acta*, A**23**, 941-958.

Li, C., Jaques, S.D.M., Chen, Y., Daisenberger, D., Xiao, P., Markocsan, N., Nylen, P. & Cernik, R.J. (2016). *J. Appl. Cryst.* **49**, 1904-1911.

Marquardt, D.W. (1970). *Technometrics*. **12**, 591-612.

Morozov, V.A. (1984). *Method for Solving Incorrectly Posed problems*. Berlin: Springer.

Press, W.H., Flannery, B.P., Teukolsky, S.A. & Vetterling, W.T. (1986). *The Art of Scientific Computing*. New York: Cambridge University Press.

Sánchez-Bajo, F. & Cumbrera, F.L. (2000). *J. Appl. Cryst.* **33**, 259-266.

Stokes, A.R. (1948). *Proc. Phys. Soc. London*, **61**, 382-391.

Stokes, A.R. & Wilson, J.C. (1942). *Math. Proc. Camb. Phil. Soc.* **38**, 313-322.

Tikhonov, A.N. & Arsenin, V.Y. (1977*). Filtz John Scripta Series in Mathematics*: *Solution of Ill-PosedPproblems*. New York: John Wiley & Sons.

Toby, B.H. & Egami, T. (1992). *Acta Cryst.* **A48**, 336-346.

Varah, J.M. (1979). *SIAM Rev*. **21**, 100-111.

Warren, B. E. (2014). *X-ray Diffraction*. New York: Dover Publications.

Wojdyr, M. (2010). *J. Appl. Cryst.* **43**, 1126-1128.